Title
MEASUREMENTS OF INTERACTION CROSS SECTIONS AND NUCLEAR RADII IN LIGHT p-SHELL REGION

Author
Tanihata, I.

Publication Date
1985-09-01

LBL-20244
Preprint c.2

Lawrence Berkeley Laboratory
UNIVERSITY OF CALIFORNIA

Submitted to Physical Review Letters

MEASUREMENTS OF INTERACTION CROSS SECTIONS AND NUCLEAR RADII IN LIGHT p-SHELL REGION

I. Tanihata, H. Hamagaki, O. Hashimoto,
Y. Shida, N. Yoshikawa, K. Sugimoto,
O. Yamakawa, T. Kobayashi, and N. Takahashi

September 1985

NUCLEAR SCIENCE DIVISION

Prepared for the U.S. Department of Energy under Contract DE-AC03-76SF00098

DISCLAIMER

MEASUREMENTS OF INTERACTION CROSS SECTIONS AND NUCLEAR RADII IN LIGHT p-SHELL REGION

I. Tanihata,* H. Hamagaki, O. Hashimoto, Y. Shida, and N. Yoshikawa

Institute for Nuclear Study, University of Tokyo,

3-2-1 Midori-cho, Tanashi, Tokyo 188 Japan,

and

K. Sugimoto,** O. Yamakawa, and T. Kobayashi

Nuclear Science Division, Lawrence Berkeley Laboratory,

University of California, Berkeley, CA 94720, USA

and

N. Takahashi

College of General Education, Osaka University

1-1 Machikaneyama, Toyonaka, Osaka 560 Japan

Abstract

Interaction cross sections(σ_I) for all the known Li isotopes (^{6}Li -^{11}Li) and ^{7}Be, ^{9}Be, and ^{10}Be on targets Be, C, and Al have been measured at 790 MeV/nucleon. Root-mean-square radii of these isotopes as well as He isotopes have been deduced from the σ_I using a Glauber-type calculation. Appreciable differences of radii among isobars (^{6}He-^{6}Li, ^{8}He-^{8}Li, and ^{9}Li-^{9}Be) have been observed for the first time. The nucleus ^{11}Li showed a remarkably large radius suggesting a large deformation or a long tail in the matter distribution.

PACS Numbers: 21.10.Gv, 25.70.-z, 27.20.+n

Recently, exotic-isotope beams, produced through the projectile-fragmentation process in high-energy heavy-ion reactions, were used to measure the interaction cross sections(σ_I) for all the known He isotopes.[1] This novel technique of using exotic nuclear beams makes it possible to study systematically properties of unstable nuclei. In the present paper, we report the σ_I for all the known Li isotopes (^{6}Li, ^{7}Li, ^{8}Li, ^{9}Li, and ^{11}Li) and ^{7}Be, ^{9}Be, and ^{10}Be on target nuclei Be, C, and Al at 790 MeV/nucleon. A firm basis has been empirically established by using a Glauber-type calculation to extract root-mean-square(rms) nuclear radii from the σ_I.

The secondary beam of ^{11}Li was produced through projectile fragmentation of the 800-MeV/nucleon ^{20}Ne primary beam. The other Li isotopes and Be isotopes were produced from a ^{11}B primary. The primary beams were accelerated by the Bevalac at the Lawrence Berkeley Laboratory. The secondary isotopes were produced in a production target of Be and were separated by rigidity using the beam-line magnet system as described in previous papers.[1,2] The rigidity separated isotopes were further identified before incidence on a reaction target by velocity (time-of-flight(TOF)) and by charge (pulse height in scintillation counters). No contamination more than 10^{-3} was observed in any selected isotope beams.

The σ_I was measured by a transmission experiment using the large acceptance spectrometer as shown in the measurement of He-isotopes.[1] Here the σ_I is defined as the total reaction cross section for the change of proton and/or neutron number in the incident nucleus. The obtained σ_I are listed in Table I. The largest systematic error on σ_I up to about 0.3 % came from uncertainties in estimating the scattering-out probability of the non-interacting nuclei. All other systematic errors were estimated to be less than 0.2 % of the σ_I.

The interaction nuclear radius R_I is defined as

$$\sigma_I(p,t) = \pi[\, R_I(p) + R_I(t)\,]^2 \quad , \tag{1}$$

where $R_I(p)$ is the projectile radius and $R_I(t)$ is the target radius. The separability of projectile and target radii assumed in the equation was examined using σ_I of various projectile-target combinations. Figure 1 shows R_I of Li and Be isotopes obtained from different targets. Here the absolute scale of the radius was determined from a least squares fitting of σ_I of ^{4}He+^{4}He, ^{9}Be+^{9}Be, ^{12}C+^{12}C, ^{4}He+^{12}C, and ^{9}Be+^{12}C reactions.[1,3,4] It is clearly seen that a projectile radius is in fact independent of target variation. As the result the assumption of the separability of projectile and target radii was demonstrated to be valid within $\pm$0.02 fm. This separability indicates that R_I is an experimentally well defined size parameter of a nucleus. Average values of R_I deduced from the Be, C, and Al targets are, therefore, used for further discussion.

In Table II the obtained R_I (column 1) are listed together with the root-mean-square(*rms*) radii R^e_{rms} of the charge distribution (column 2) determined by electron scattering experiments.[5] The dependence of R_I on the mass-number(A) and that of R^e_{rms} show a noticeable difference, i.e., R_I increases with A whereas R^e_{rms} stays almost constant for $A \geq 6$. We will now show that the differences are due to the different definitions of the two kinds of radii and not due to the difference between the charge and the nuclear distributions.

We relate the σ_I to the *rms* radius by a Glauber-type calculation using Karol's prescription[6] and show that the *rms* radius of nuclear-matter distribution can be determined independently from assumed model density functions. To examine the functional dependence, we employed three types of nuclear density distributions; a Gaussian[6], a shell-model harmonic oscillator,[7] and a droplet model[8] with Yukawa folding function ($\frac{1}{r}e^{-r/b}$). The Gaussian and the harmonic-oscillator distributions have only one size parameter a_G and a_{ho}, respectively. On the other hand, the droplet-model distribution has two parameters; a size parameter r_0 and a diffuseness parameter b. In the following we discuss how the *rms* radius can be deduced using the Gaussian and the harmonic-oscillator distribution and show that the *rms* radii obtained from these two distributions are equal. We also show that the droplet-model distribution gives equivalent results.

In a Glauber-type calculation nucleon-nucleon(NN) cross sections have to be given. The free NN cross sections are, however, inappropriate because the effective values may differ from the free nucleon values due to nuclear-matter effects. In fact, it has been reported that the mean free path of the 800-MeV protons inside the nuclear matter was longer than expected from the free NN cross sections[9] and also that the effective values of NN cross sections were smaller in uranium reactions at 900 MeV/nucleon.[10] To determine the effective values of NN cross sections for the present analysis, the calculations were first made for collisions of identical stable isotopes, i.e., $^{4}He+^{4}He$, $^{6}Li+^{6}Li$, $^{7}Li+^{7}Li$, $^{9}Be+^{9}Be$, and $^{12}C+^{12}C$. The width parameter a_G (or a_{ho}) and a scaling factor of NN cross sections were taken as the fitting parameters in order to fit both of the R^{e}_{rms} and the σ_I.

It was found that the effective values of NN cross sections which were 80 % of that of free nucleons gave a good fit in the present mass range. In Fig. 2, the *rms* radii R^{G}_{rms} obtained after fitting the σ_I using the Gaussian distribution with the effective NN cross sections are shown by the dashed line. The solid line in the figure indicates the charge *rms* radii R^{c}_{rms} obtained in the same way using the harmonic-oscillator distribution. It is seen that the R^{e}_{rms} are well reproduced with the fixed values of effective NN cross sections. It is also noted that the difference between the R^{e}_{rms} of ^{6}Li and ^{7}Li is reproduced by the harmonic oscillator distribution because of the occupation number difference between protons and neutrons.

Having established that the *rms* radius derived from σ_I agrees with R^{e}_{rms}, we now extend the calculations to unstable nuclei using the effective NN cross sections. Column 4 in Table II shows the deduced R^{G}_{rms} and columns 5-7 show *rms* radii deduced using the harmonic-oscillator distribution (R^{m}_{rms}, matter radius; R^{c}_{rms}, charge radius; and R^{n}_{rms}, neutron matter radius). The R^{G}_{rms} and the R^{m}_{rms} agree well for each nucleus.

Calculations using the droplet model gave further evidence that different distributions can give essentially the same values for *rms* radii. In this model we have two parameters, a size parameter (r_0) and a diffuseness parameter (b), and a given σ_I can give a locus in the r_0–b plane instead of a unique determination of two parameters. A constant R^m_{rms} also gives another locus. It was found that these two loci lay almost in parallel over a wide range. For example in ^{9}Be, a change of b from 0.4 to 0.8 fm affects R^m_{rms} only by 0.025 fm under the fixed σ_I. Consequently the R^m_{rms} was determined rather independently of the selected value of b (or r_0). The R^m_{rms} were calculated, using the value of b from 0.4 to 0.8 fm[12], for ^{4}He, ^{6}Li, ^{9}Be, and ^{12}C and were found to be equal within 0.04 fm to those obtained using the harmonic oscillator. This situation can be understood intuitively because both σ_I and R^m_{rms} are sensitive to the surface region of the nuclear density.

From the preceding discussion we concluded that the nuclear matter radii deduced from σ_I were insensitive to the selection of the model density distribution. Figure 3 shows the R^m_{rms} determined using the harmonic oscillator distribution. For the first time, we observed appreciable differences of radii between pairs of isobars with different isospin, ^{6}He-^{6}Li, ^{8}He-^{8}Li, and ^{9}Li-^{9}Be. The larger radii of the neutron rich isotopes ^{6}He and ^{8}He, which have only two protons, suggest the existence of thick neutron skins. The large neutron skins are also seen as a differences between R^c_{rms} and R^n_{rms} in Table II. On the other hand, a pair of mirror nuclei ^{7}Li - ^{7}Be show the same matter radius.

It is interesting to note that the nucleus ^{11}Li, with the neutron number of p-shell closure in the naive shell model, shows a considerably larger radius than neighboring nuclei. It suggests the existence of a large deformation or of a long tail in the matter distribution due to the weakly-bound nucleons. A weakly-bound nucleon may enhance the σ_I because it could be kicked out from the nucleus with a small momentum transfer. A rough estimation of the excitation-energy distribution of nucleons after a nucleon-nucleon collision, however, showed that the change in separation energy from 10 MeV to zero affect the σ_I by only about 3 %. This binding effect, therefore, can not explain the bulk of the observed deviation.

In summary, we have measured the interaction cross sections σ_I of nucleus-nucleus collisions using the secondary beams of unstable and stable Li and Be isotopes. The interaction nuclear radii R_I of these nuclei have been determined from the σ_I. The observed separability of R_I between projectile and target indicated that the R_I is a well defined size parameter of a nucleus. The matter *rms* radii was deduced using three model density distributions: a Gaussian, a shell-model harmonic oscillator, and the droplet model; as a result three distributions gave essentially the same *rms* radii. This method of radius measurement has been shown to agree with electron scattering for stable nuclei. It has been observed that the radius of ^{11}Li is much larger than other neighboring nuclei presented here. It suggests the existence of a large deformation or a long tail in the matter distribution. The differences between the matter *rms* radii R^m_{rms} for isobars of different isospins, ^{6}He-^{6}Li, ^{8}He-^{8}Li, ^{9}Li-^{9}Be, have been observed for the first time. A pair of mirror nuclei ^{7}Li - ^{7}Be have been found to have equal R^m_{rms}.

We would like to thank Y. Matsuyama, T. Fujino, F. S. Bieser for their technical assistance. Discussions with Dr. D. E. Greiner and Dr. W. D. Myers are gratefully acknowledged. This work was supported by the Director, Division of Nuclear Physics of the Office of High-Energy and Nuclear Physics of the US DOE under Contract DE-AC03-76SF00098, the INS-LBL Collaboration Program, and by the Japan-US Joint Program for High-Energy Physics. One of the author (I.T.) gratefully acknowledges the support of Yamada Science Foundation.

References

* also, Lawrence Berkeley Laboratory, University of California.

** Permanent address, Faculty of Science, Osaka University.

1. I. Tanihata et al., Physics Letters, in press.

2. I. Tanihata, Hyperfine Interactions **21,** 251 (1985).

3. J. Jaros et al., Phys. Rev.C **18,** 2273 (1978).

4. H. H. Heckmann et al., Phys. Rev.C **17,** 1735 (1978).

5. R. C. Barrett and D. F. Jackson, *Nuclear Sizes and Structure,* Clarendon press, Oxford 1977, p146.

6. P. J. Karol, Phys. Rev.C **11,** 1203 (1975).

7. L. R. B. Elton, *NuclearSizes* , Oxford University Press 1961, p21.

8. W. D. Myers and K. -H. Schmidt, Nuclear Physics **A410,** 61 (1983).

9. I. Tanihata, S. Nagamiya, S. Schnetzer, and H. Steiner, Phys. Lett. **100B,** 121 (1981).

10. D. E. Greiner et al., Phys. Rev.C **31,** 416 (1985).

11. Here σ_I(^{6}Li,^{6}Li) and σ_I(^{7}Li,^{7}Li) were not directly measured but calculated from the R_I(^{6}Li) and R_I(^{7}Li) using Eq. (1). These values were estimated to be reliable within a few % using the projectile-target separability discussed above.

12. Commonly accepted value of b is $\approx$0.7 for an $A>10$ stable nucleus and $\approx$0.4 for ^{4}He. J. Friedrich and N. Voegler, Nuclear Physics **A373,** 192 (1982).

Table I. Interaction cross sections(σ_I)
σ_I in mb

beam	target Be	C	Al
^{6}Li	651± 6	688±10	1010±11
^{7}Li	686± 4	736± 6	1071± 7
^{8}Li	727± 6	768± 9	1147±14
^{9}Li	739± 5	796± 6	1135± 7
^{11}Li		1040±60	
^{7}Be	682± 6	738± 9	1050±17
^{9}Be	755± 6	806± 9	1174±11
^{10}Be	755± 7	813±10	1153±16

Table II. The interaction nuclear radii and the rms radii (fm)

		e-scat.	Gaussian	harmonic oscillator		
	R_I	R^e_{rms}	R^G_{rms}	R^m_{rms} *	R^c_{rms} *	R^n_{rms} *
^{4}He	1.41±0.03	1.67±0.01	1.72±0.06	1.72±0.06	1.72±0.06	1.72±0.06
^{6}He	2.18±0.02		2.75±0.04	2.73±0.04	2.46±0.04	2.87±0.04
^{8}He	2.48±0.03		2.70±0.03	2.69±0.03	2.33±0.03	2.81±0.03
^{6}Li	2.09±0.02	2.56±0.10	2.54±0.03	2.54±0.03	2.54±0.03	2.54±0.03
^{7}Li	2.23±0.02	2.41±0.10	2.50±0.03	2.50±0.03	2.43±0.03	2.54±0.03
^{8}Li	2.36±0.02		2.51±0.03	2.51±0.03	2.41±0.03	2.57±0.03
^{9}Li	2.41±0.02		2.43±0.02	2.43±0.02	2.30±0.02	2.50±0.02
^{11}Li	3.14±0.16		3.27±0.24	3.27±0.24	3.03±0.24	3.36±0.24
^{7}Be	2.22±0.02		2.48±0.03	2.48±0.03	2.52±0.03	2.41±0.03
^{9}Be	2.45±0.01	2.52±0.01	2.49±0.01	2.50±0.01	2.47±0.01	2.53±0.01
^{10}Be	2.46±0.03		2.38±0.02	2.39±0.02	2.34±0.02	2.43±0.02
^{12}C	2.61±0.02	2.45±0.01	2.40±0.02	2.43±0.02	2.43±0.02	2.43±0.02

*Superscripts m ,c , and n indicate the nuclear matter, the charge, and the neutron matter distributions, respectively.

Figure Captions

Fig.1 The R_I are plotted for Li and Be isotopes. The values obtained by three different targets agree with each other showing the separability of projectile and target R_I.

Fig.2 The charge *rms* radii are plotted. Circles indicate the radii R^e_{rms} determined by electron scatterings. The dashed line shows the result obtained by fitting the σ_I using a Glauber-type calculation employing the Gaussian density distribution. The solid line shows the result obtained using a shell-model harmonic-oscillator distribution.

Fig.3 The matter *rms* radius R^m_{rms}. Lines connecting isotopes are only guides for eyes. Differences in radius are seen in isobars with A =6,8, and 9. The radius of ^{11}Li is much larger than that of other nuclei.

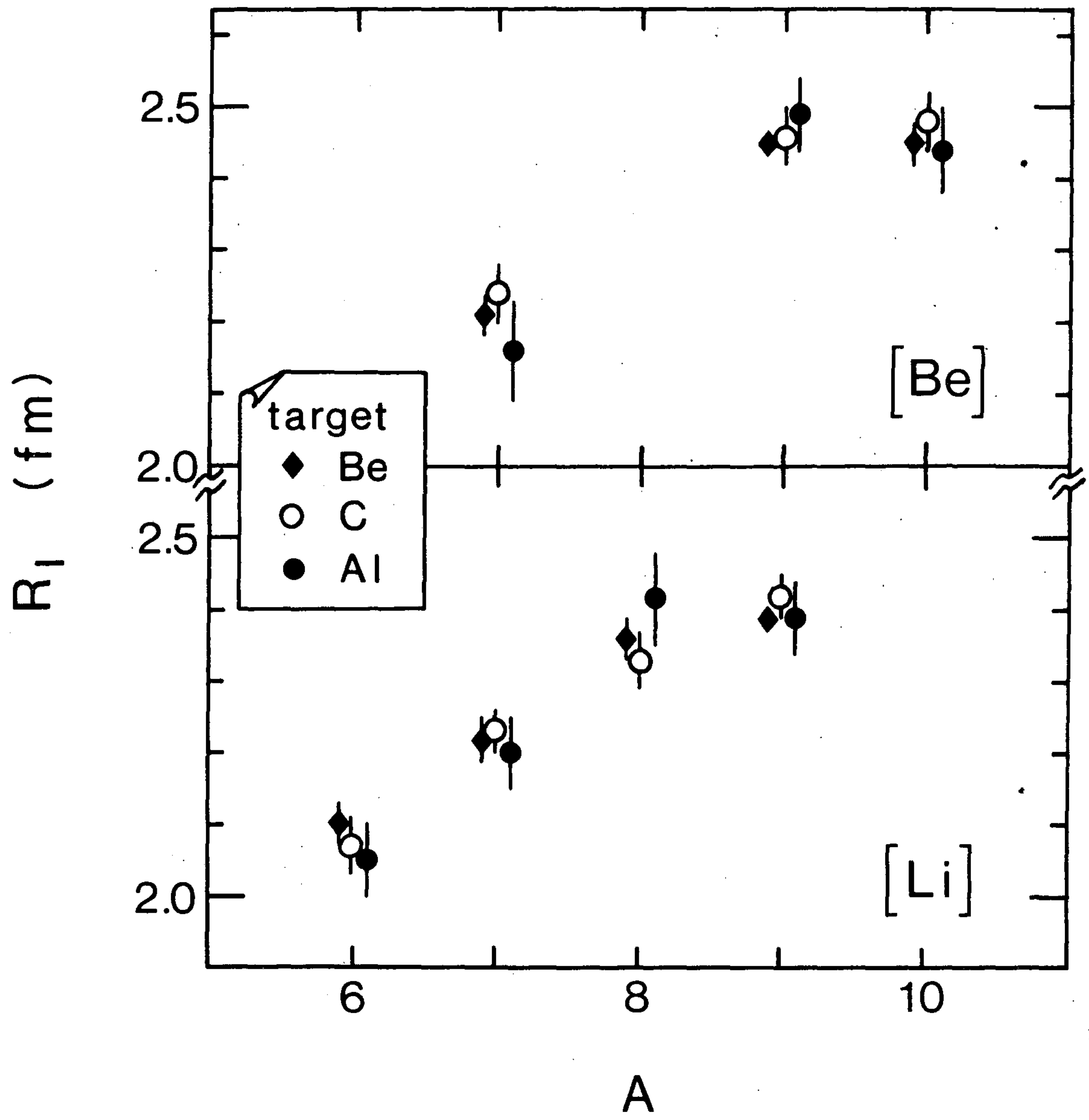

XBL 858-3499

Fig. 1

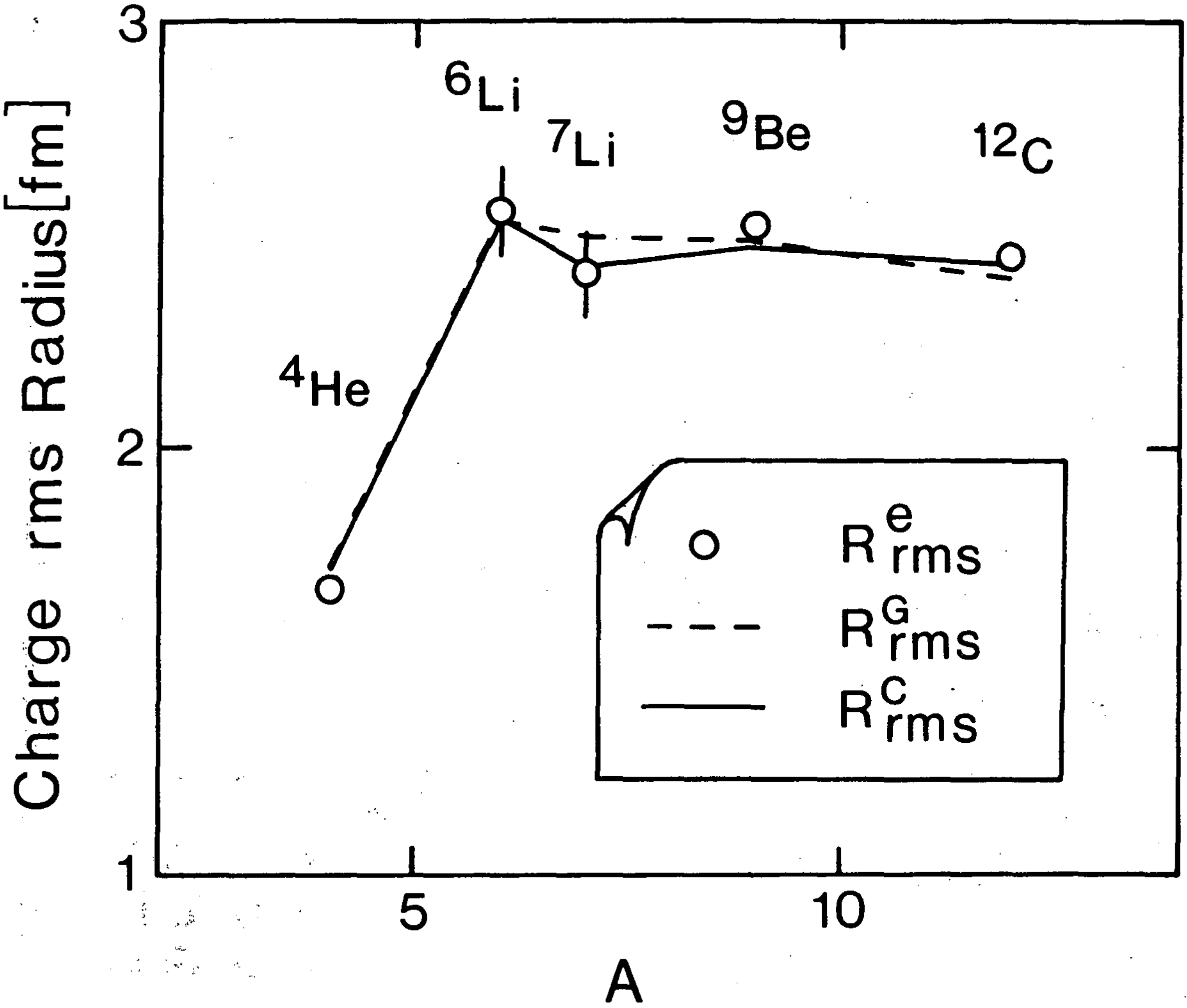

XBL 858-3498A

Fig. 2

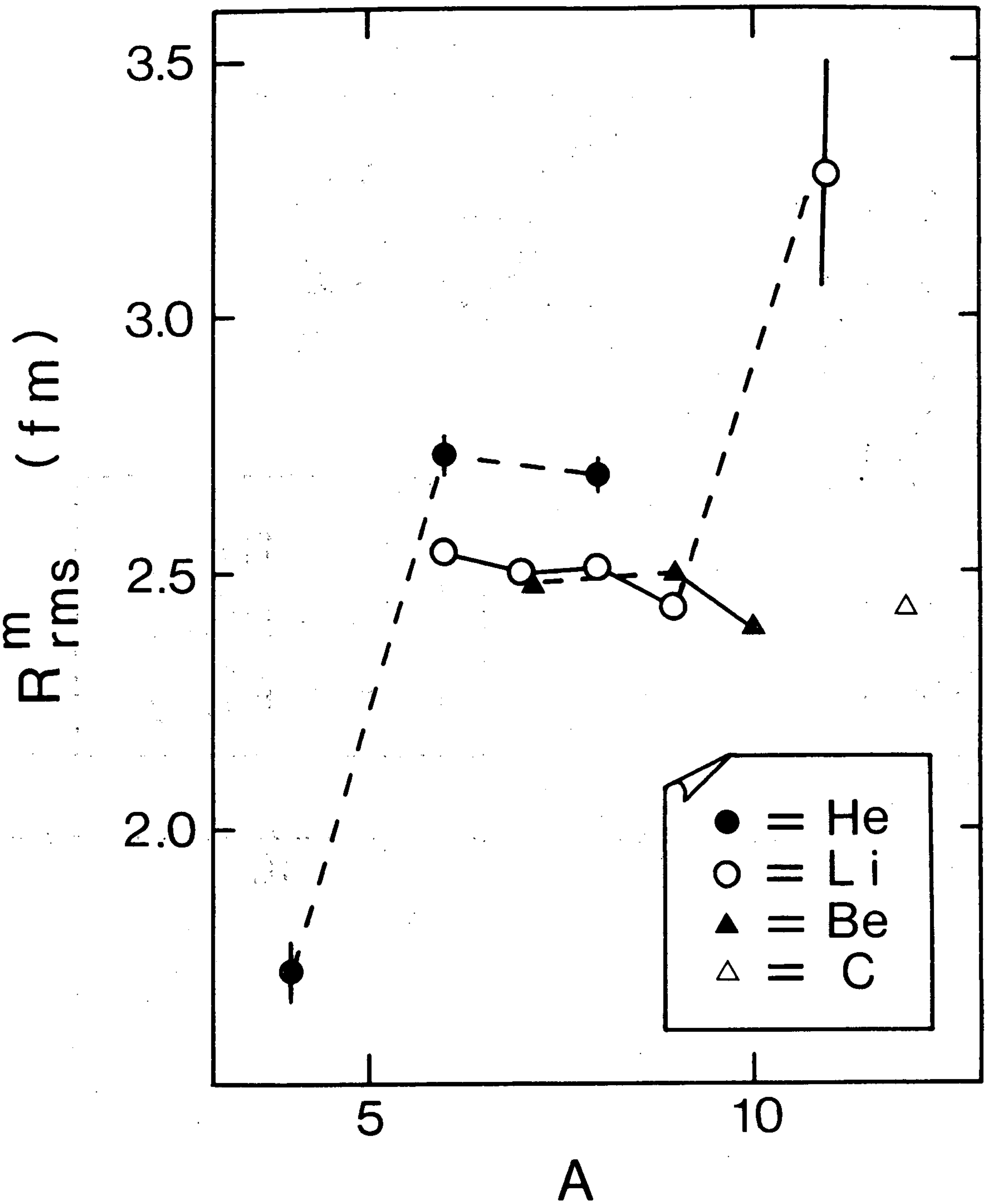

XBL 858-3500

Fig. 3